Semiautomated Isochoric Apparatus for $p-V-T$ and Phase Equilibrium Studies

Lâle Yurttaş, James C. Holste, and Kenneth R. Hall*

Department of Chemical Engineering, Texas A&M University, College Station, Texas 77843

Bruce E. Gammon and Kenneth N. Marsh

Thermodynamics Research Center, The Texas A&M University System, College Station, Texas 77843

A compact, semiautomated isochoric apparatus is described. This apparatus can be used to measure $p-V-T$ properties, vapor pressures for pure compounds, and phase boundaries for mixtures at temperatures between 200 and 450 K and pressures up to 18 MPa. A highly reproducible diaphragm-type differential pressure transducer is an integral part of the isochoric cell, providing pressure measurements precise to ±0.01%. The precision of the temperature measurement is ±0.001 K. A microcomputer controls the temperature, records measured temperatures and pressures, and processes and stores the information. The performance of the apparatus is tested by measurements of the vapor pressure and isochores for carbon dioxide.

Introduction

$p-V-T$ studies on fluids over a wide range of temperature and pressure allow the calculation of the $p-V-T$ surface with the derivative thermodynamic functions and phase behavior. Equations of state provide thermodynamic properties of fluids from a minimum of experiments, but accurate and internally consistent measurements are essential to develop good equations of state. Numerous equations of state have been proposed; however, few accurate, wide-range $p-V-T$ measurements exist for mixtures to test and improve such models.

Several methods exist to measure $p-V-T$ properties for pure components and their mixtures. An accurate method, introduced by Burnett (*1*), does not require measurements of mass or volume; instead, densities are inferred by data reduction (*2–4*) from accurate isothermal pressure measurements made before and after stepwise expansions between two volumes.

The isochoric method is another high-precision technique for obtaining $p-V-T$ results. This method involves charging into a known volume a sample of known mass and measuring the pressure at a sequence of temperatures. The Burnett apparatus has also been used in the isochoric mode (*6–8*) as suggested by Burnett (*5*). These Burnett–isochoric experiments consist of performing isochoric runs after an expansion in a Burnett run at some base temperature as indicated in Figure 1. Phase boundaries can be determined from the discontinuity in the slopes of the isochores. The Burnett–isochoric method has been used at Texas A&M University (*9–16*) to determine accurate densities and phase boundaries. Measurements with this technique in the liquid region, however, are time-consuming and tedious.

In the various isochoric methods (*17–23*), the pressure is measured as a function of temperature along a nearly isochoric path (pseudoisochores), to give the two-phase loci, $(\partial p/\partial T)_\rho$ and $(\partial^2 p/\partial T^2)_\rho$, which are used to calculate the residual thermodynamic functions. Precise densities are assigned to each isochore, using density measurements made on the same fluid along an isotherm using either the Burnett method (*14*) or a pycnometer (*24*). The method described here uses mixtures of gravimetrically prepared compositions and does not require measurements of the mass and volume of the actual sample. The method does require a knowledge of the density over a pressure range at one temperature.

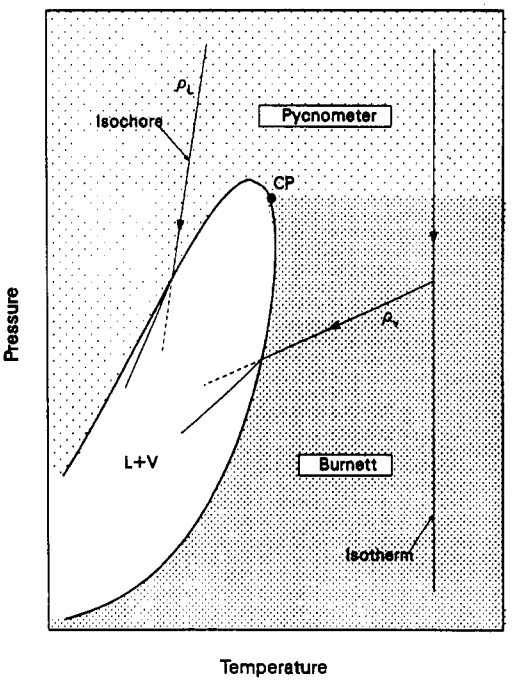

Figure 1. $P-T$ phase diagram for a mixture. The regions in which the Burnett apparatus and pycnometer are the instruments of choice for isothermal density measurements are shown.

The principal features of the apparatus described include a compact and simple design, small sample size, built-in differential pressure transducer, and homogeneous temperature distribution. The simple design of the isochoric apparatus allows automation; a microcomputer is employed for temperature control and data acquisition. A single sample can be used for measurement of the $p-V-T$ surface over the entire fluid region, minimizing the possibility of sample contamination. Changes of temperature and subsequent establishment of thermal equilibria are rapid. The apparatus can be operated at temperatures between 200 and 450 K and pressures up to 18 MPa. Measurements on carbon dioxide have been used to check the correct operation of the apparatus.

0021-9568/94/1739-0418$04.50/0

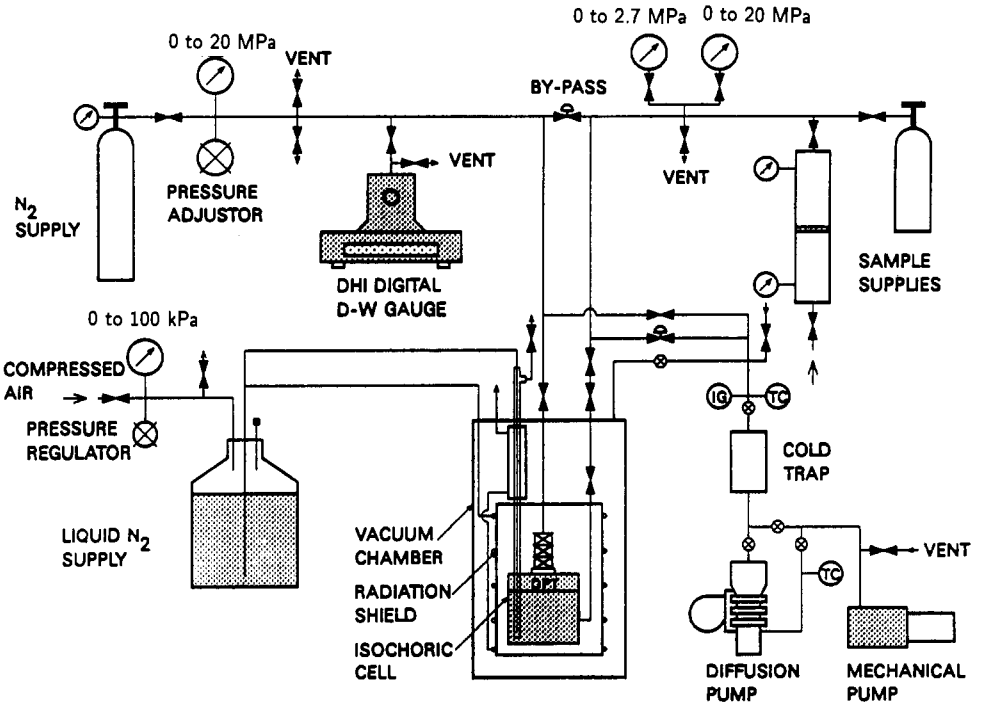

Figure 2. Schematic diagram of the isochoric apparatus.

Experimental Section

Apparatus. The schematic of the apparatus is shown in Figure 2. The essential elements are an isochoric cell with a vacuum chamber, a semiautomated pressure measurement system, an automated temperature control and measurement system, a gas manifold system, a cooling system, and a vacuum system.

The fluid in the sample cell is isolated from the sample lines by a valve and from the external pressure measurement system by a metal diaphragm which is the pressure-transmitting element of a built-in diaphragm-type differential pressure transducer (DPT). The pressure of the internal fluid is obtained indirectly by measuring the pressure of the counterbalancing gas with a digital dead-weight gauge and a barometer when the diaphragm is in the null position.

A sectional view of the isochoric apparatus is shown in Figure 3. The apparatus is designed to allow rapid change and restabilization of temperatures, temperature control to better than ±0.001 K, and temperature gradients across the cell of less than ±0.003 K. The cell is constructed from a high-strength beryllium–copper alloy (Be–Cu 175), having a high thermal conductivity. Yurttaş (*25*) discusses details of the apparatus design. To minimize adsorption, the inner surfaces of the cell were polished and then gold-plated, and a gold-plated metal c-ring was used to seal the bottom plate to the main body of the sample cell. Special considerations were also made to reduce energy loss, provide sample agitation, and establish adequate cooling.

Pressure Measurement System. The sample volume is separated from the external pressure gauges by a DPT, designed as an integral part of the isochoric cell (Figure 3). An inert gas, N_2, is used as the medium between the dead-weight gauge (DWG) and the diaphragm. The absolute accuracy in the pressure is limited primarily by the dead-weight gauge; the gauge employed provided measurements accurate to ±0.01% or better. Commercial pressure transducers which could be mounted directly in the cell, thereby eliminating the DPT and the intermediate fluid, either are limited in the temperature range or provide an inadequate accuracy.

The DPT, which incorporates design criteria developed at Texas A&M University over the past decade (*25–27*), consists

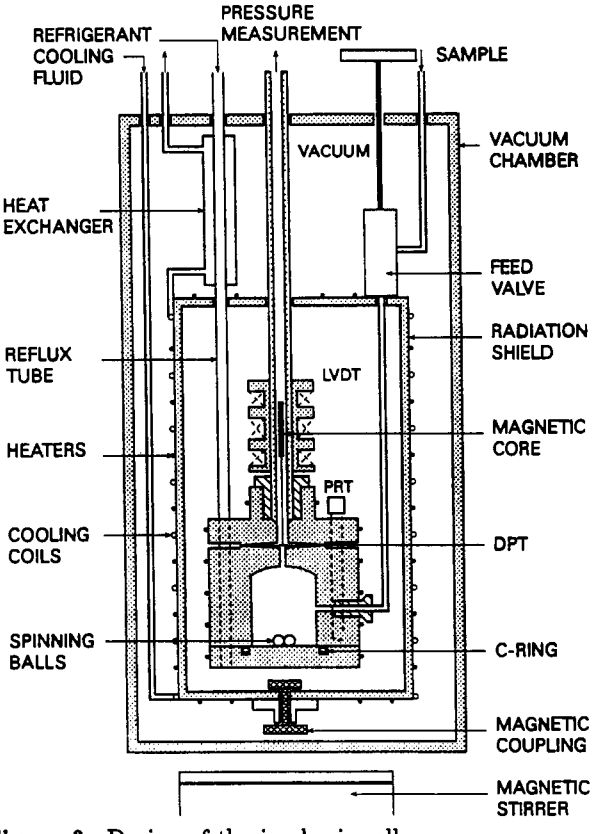

Figure 3. Design of the isochoric cell.

of a stainless steel diaphragm (0.05 mm thick) as the pressure-transmitting element, the transducer body, and a linear variable differential transformer (LVDT) for detecting deflections of the diaphragm. In this design, the coils are mounted exterior to the pressure wall, so that no electrical leads enter the high-pressure chamber. The details of the electrical circuit and the measurement techniques have been reported previously (*28*).

Because the DPT is designed to sense small differences in moderate pressure systems and to have negligible effect on the precision and accuracy of the pressure measurements,

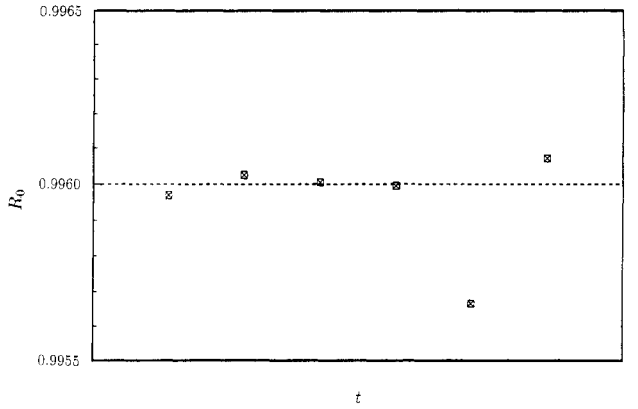

Figure 4. Stability of the transducer null value over a period of time t of seven months at T = 325 K and p = 0.665 MPa. δR_0 = 0.0001 corresponds to 0.1 kPa.

excellent reproducibility of the null position of the diaphragm (Δp = 0) and high sensitivity are required. The stability of the null position is demonstrated in Figure 4, which shows the ratio transformer settings (R_0) at null pressure difference obtained at irregular intervals over a period of seven months. The only measurements differing by more than 0.1 kPa from the initial value occurred after the formation of a polymeric layer on the diaphragm as the result of the decomposition of a compound in the cell.

The null reading depends on the temperature and pressure in the system, and calibration indicates that the pressure dependence of the null position is slightly smaller than the accuracy of the dead-weight gauge; therefore, its effect is negligible. The temperature dependence is slightly larger, but reproducible to ±0.1 kPa.

Because the output of the DPT, R, varies linearly with the pressure difference over a modest pressure range (*28*) (at least ±20 kPa for this device), the DPT can be used to interpolate between convenient DWG readings. The value (p_0) determined from the linear fit to five external pressures (p_{ex}) corresponds to a pressure reading taken with the diaphragm in the exact null position (R_0), $p_{ex} = p_0 + S(R - R_0)$; therefore, no volume correction for diaphragm displacement is necessary. This method is much more convenient and much higher resolution is achieved compared to the conventional technique, which requires that the measurement be made with a null pressure difference across the diaphragm. The sensitivity of the diaphragm is determined independently during each sample pressure measurement (*28*), thereby providing a check on the reproducibility. The stability and resolution (S) of the pressure measurements are limited by the compressibility of the internal fluid. For vapors the pressure resolution exceeds 0.01 kPa for a five-digit resolution in the ratio transformer setting. For liquids the apparent sensitivity can be as low as 1.5 kPa, depending on the compressibility of the sample.

The absolute pressure measurements are made with a DH Instruments digital dead-weight gauge (DWG), model 26410, and a mercury barometer (Figure 2). The dead-weight gauge consists of a piston–cylinder assembly to transform a pressure p into a force F proportional to a piston–cylinder effective area A by the relation $F = pA$ and a commercial balance which measures and gives a digital value for the force F. The electronic balance measures force from 0 to 98 N (the weight of a mass of 10 kg) and displays the force value with a resolution of 10^5 counts. This gauge has three piston–cylinder assemblies for 0–1-, 0–5-, and 0–50-MPa pressure ranges, the stated accuracy of the gauge being ±(5 counts + 0.005% of reading). An IEEE 488 data interface allows for automatic data acquisition. Measured pressures are corrected for piston–cylinder temperature changes using a platinum resistance thermometer (PRT) located inside the piston–cylinder assembly. The balance is zeroed at atmospheric pressure before the pressure measurements, and the resulting pressures are corrected for the local gravitational acceleration. Atmospheric pressures are measured to ±0.003 kPa using an Ideal-Aerosmith Inc. (model 11-11-60) mercury barometer.

Temperature Control and Measurement System. Because temperatures must be controlled precisely during long equilibration times, a digital control on the aquisition system (*23*, *29*) shown in Figure 5 was used (*25*). Temperature is measured with a Leeds and Northrup 25-Ω platinum resistance thermometer mounted directly on the cell. The four-lead PRT was calibrated by the manufacturer (traceable to NIST). If R_T is the resistance of the PRT, V_T the voltage drop across the thermometer, and V_S is the voltage drop across a standard resistor R_S in series with the thermometer, then $R_T = (V_T/V_S)R_S$. The temperatures on the radiation shield are measured by four Weed 100-Ω PRT's and a thermopile.

The temperature control algorithm consists of two parts: (1) a proportional controller which brings the cell temperature within 0.5 K of the desired temperature and (2) a proportional and integral controller, tuned for small temperature differences, which provides convergence to within <0.001 K of the desired temperature. After the desired temperature is attained, about 90% of the energy required for maintaining the temperature of the cell is delivered to the radiation shield. After equilibrium is established, the computer performs the data acquisition and partial data analysis.

Experimental Procedure. Incomplete degassing of the sample is a potential source of error in vapor pressure or phase boundary measurements using a static method. Degassing is carried out by repeated cycles of freezing and melting under vacuum until a pressure of less than 1 mPa is obtained over the frozen solid at liquid nitrogen temperature. The samples then are distilled from the supply cylinder into the isochoric cell, where they are condensed at an appropriate temperature. As a test for purity, the vapor pressure of a given sample at a fixed temperature is measured at different overall densities (*i.e.*, different liquid-volume fractions). A variation of the vapor pressure with the number of expansions indicates the presence of impurities. The change in the vapor pressure should be less than the measurement errors for several consecutive expansions. Any remaining noncondensibles can be removed from the cell by expanding the vapor phase into an evacuated volume until no change is observed in the measured vapor pressure.

The first step in an isochoric run is to evacuate the sample lines and the cell to less than 0.1 kPa. The cell is then flushed several times with the measurement fluid, and a sample of the fluid is then loaded into the cell as a single phase (either vapor or liquid). For dew- and bubble-point measurements on mixtures, extreme caution must be taken to avoid phase separation during the transfer process. After the transfer process is completed and the feed valve is closed, sufficient time is allowed for temperature equilibration.

Five pressures are measured around the null point of the DPT. The only variables recorded manually are the ratio transformed settings which are entered into the computer when prompted. The pressure and ratio transformer setting pairs are fitted to a straight line by regression, and the pressure (p_0) corresponding to the null setting (R_0) of the DPT is calculated. Next, the set point is changed and the procedure repeated. Usually the temperature of the system is initially set at the highest value of interest and then lowered to obtain the pseudoisochoric measurements at evenly spaced temperatures. In this manner, a series of pressure–temperature determinations is made on a constant-mass sample.

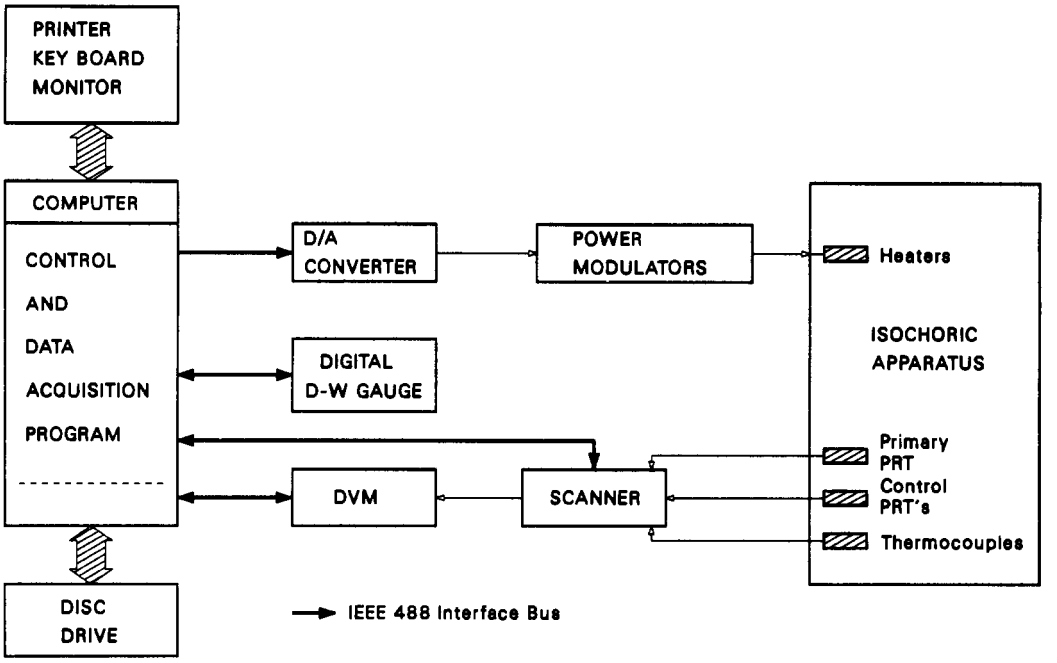

Figure 5. Diagram for the digital computer control and data acquisition.

The isochoric measurements are usually carried into the vapor–liquid region. In this region, the use of a magnetic stirrer accelerates phase equilibrium. The stirrer is turned off before each pressure measurement. After measuring an isochore, a second pressure measurement at the initial temperature provides a test for leaks or composition changes in mixtures of unstable samples. A new density is established by expanding the sample into an evacuated section of the inlet tubing. Then the feed valve is closed, and isochoric measurements are repeated on the remaining mass of sample. In principle, a single loading at the highest density is sufficient to cover the majority of the p–V–T surface. However, several loadings at different densities provide an internal consistency check on the sample loading procedure and additional tests for decomposition or separation effects during expansion.

Results

Cell Volume Distortions. Before starting any measurement, the pressure and temperature dependences of the volume of the cell and the associated tubing were calibrated over the temperature and pressure range of interest using pure CO_2. First we measured two vapor isochores; the densities along the isochores were calculated using the CO2PAC program package developed by Ely et al. (*30*). This equation of state provides densities accurate to 0.1%. These two isochores, as well as others which are used for a later calibration, are shown in Figure 6. The temperature and pressure dependence of the effective cell volume is $V/V_0 = 1 + (5.264 \times 10^{-5}\ K^{-1})(T - T_0) + (2.727 \times 10^{-11}\ Pa^{-1})(p-p_0)$. The pressure coefficient is similar to the value reported by the supplier for the elastic modulus of Be–Cu 175, while the measured thermal expansion term differs by approximately 10% from the suppliers' value. Later, another volume calibration provided a thermal expansion coefficient of $4.663 \times 10^{-5}\ K^{-1}$ which is 24% removed from the value reported by the supplier. These disagreements may have resulted from the precipitation of the beryllium–copper alloy at elevated temperatures. However, the present values are in good agreement (<1% different) with the values reported by Lau (*24*) and show the same variation with aging of the alloy.

CO_2 Measurements. To verify the performance of the apparatus, we measured the vapor pressures of CO_2 and compared them with those calculated from the equation of state for CO_2 developed by Ely et al. (*30*). Our vapor pressure values agree with the equation of state to within ±0.04% (Table 1). From a survey of their own and other accurate measurements, Sengers and Chen (*31*) concluded that the best values of p^σ for CO_2 at 273.15 K lie in the range 3.4850

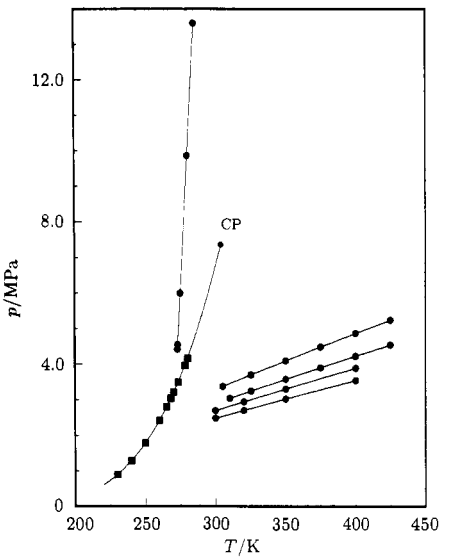

Figure 6. CO_2 vapor pressure curve and liquid and vapor isochores used in the volume calibration of the cell with respect to temperature and pressure. CP is the critical point.

Table 1. Vapor Pressure of CO_2, p^σ, and Comparison with the Value Calculated from the Equation of State of Ely et al. (*30*), p^σ_{eq}

T/K	p^σ/MPa	p^σ_{eq}/MPa	$10^2(p^\sigma - p^\sigma_{eq})/p^\sigma$
229.888	0.8896	0.889 60	+0.0000
230.000	0.8934	0.893 34	+0.0008
239.932	1.2804	1.279 90	+0.0039
249.901	1.7799	1.779 60	+0.0017
268.000	3.0336	3.033 04	+0.0020
270.000	3.2030	3.202 98	0.0000
273.150	3.4847	3.485 00[a]	−0.0009
278.000	3.9531	3.953 72	−0.0015
280.000	4.1593	4.160 15	−0.0020

[a] 3.4850 ± 0.0003 MPa by Sengers and Chen (*31*).

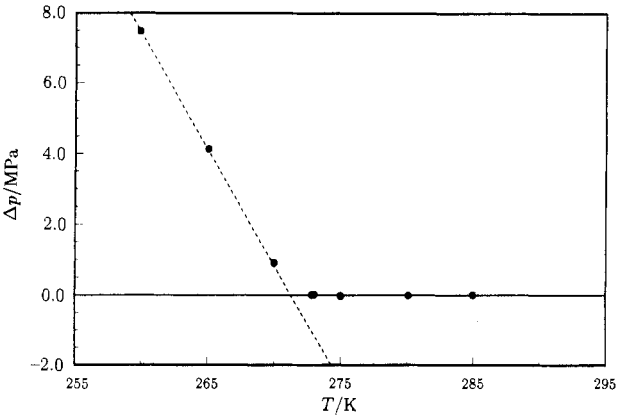

Figure 7. Difference between the measured pressures and a cubic equation, $p = a + bT + cT^2$, fitted to the single-phase results for a high-density (liquid) isochore (Table 2). The intersection of the dotted line (extrapolation of the two-phase measurements) and the zero line is the phase boundary.

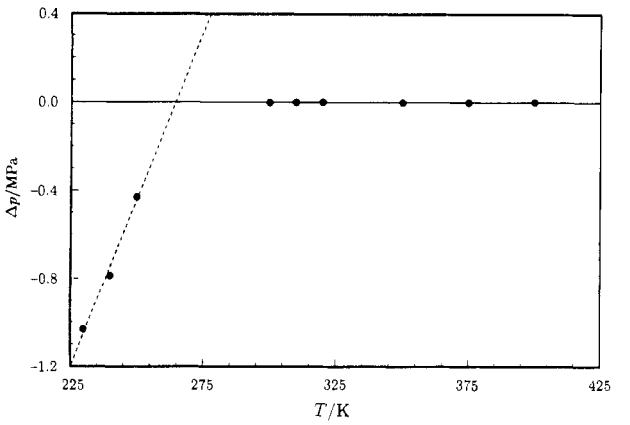

Figure 8. Difference between the measured pressures and a cubic equation fitted to the single-phase data for a low-density (vapor) isochore (Table 2). The intersection of the dotted line (extrapolation of the two-phase measurements) and the zero line is the phase boundary.

Table 2. Temperature and Pressure for CO_2 Isochores shown in Figures 7 and 8

vapor isochore		liquid isochore	
T/K	p/MPa	T/K	p/MPa
229.888	0.8896	259.858	2.4135
239.932	1.2804	265.032	2.7986
249.901	1.7800	270.009	3.2093
299.969	2.9112	272.852	4.4117
300.002	2.9119	273.023	4.5418
309.956	3.0496	275.007	5.9886
319.993	3.1868	280.111	9.8584
350.014	3.5868	284.977	13.5982
375.041	3.9140		
400.110	4.2364		

± 0.0003 MPa. Our result agrees with this value, and the equation of state is within ±0.01% of that value (Table 1). For these measurements, we used ultrapure grade CO_2 (better than 99.99 mol% purity) which was degassed by repeated cycles of freezing, pumping, and melting.

The capabilities of the apparatus are further illustrated by the measurement of a liquid and a vapor isochore for CO_2. The points of intersection (p, T) of the isochores in the single- and two-phase regions, fitted independently by least squares, give the phase boundaries precisely. For a one-component fluid, the intersection of the isochore with the vapor pressure curve determines a point on the coexistence curve. The results of the measurements along the two isochores are given in Table 2 and shown in Figures 7 and 8 which give the deviations of the measured pressures from a polynomial fit to the single-phase values. A sharp change in the slope, (dp/dT), occurs at the phase boundary. The pressure in the two-phase region can be approximated by $\ln p = A + B/T$. For temperatures up to 5–15 K away from the phase boundary, the above equation provides an adequate description of the results. The scatter in the measured pressures is no more than ±0.2% for the liquid and ±0.01% for the vapor and the two-phase regions from the corresponding representations as shown in Figure 9.

Performance and Discussion

The principal factor limiting the accuracy of our pressure measurements is the differential pressure transducer (DPT). Pressure measurements are good, but $dp = (\partial p/\partial T)_V\, dV + (\partial p/\partial V)_T\, dp$, and since both derivatives are large in the compressed liquid, small movements in the DPT affect dV and hence dp. The stability and resolution of measurements are limited by the compressibility of the fluid under study.

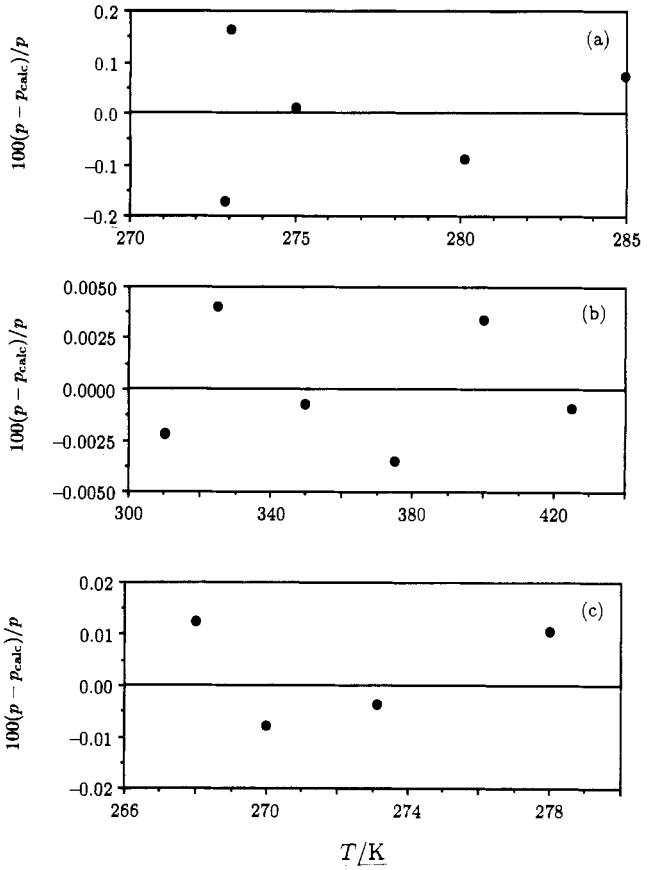

Figure 9. Relative differences between the experimental pressures and (a) a cubic equation representation of $p(T)$ fit to the high-density (liquid) isochore, (b) a cubic equation fit to the low-density (vapor) isochore, and (c) a fit of $\ln p = A + B/T$ to the two-phase measurements.

For vapors we obtained resolutions of less than 10 Pa in pressure for a five-digit resolution in the ratio transformer setting (*25*). The transducer null value is a small function of the temperature and is slightly pressure dependent. The stability of the DPT null value (at 325 K and 0.665 MPa) over a period of seven months with different fluids on the sample side of the diaphragm is shown in Figure 4. The reproducibility of the transducer is usually better than ±0.1 kPa. Unidirectional overloads as large as 18.0 MPa can be tolerated without hysteresis. In Figure 4, the changes outside the range of ±0.1 kPa were caused by sample decomposition which deposited polymeric compounds on the diaphragm. The

maximum uncertainties in pressure measurements, determined as deviations from the linear fit of the pressure ratio–transformer pairs, vary from ±0.001 to ±0.1% depending upon the compressibility of the fluid in the cell.

A microcomputer is used for both temperature control and data acquisition. After a significant temperature change, equilibrium is established within 2–3 h for temperatures above ambient. Equilibration time is usually longer for temperatures below ambient. A trim heater is used to maintain a temperature difference across the cell at less than ±0.001 K at equilibrium. The overall precision of the temperature measurement is ±0.001 K.

The vapor pressure of carbon dioxide has been measured, and comparison with literature values shows an accuracy of better than ±0.04%. The feasibility of obtaining dew and bubble points of a mixture of constant composition has been shown by measurements on two isochores for carbon dioxide in the high- and low-density regions.

Literature Cited

(1) Burnett, E. S. *J. Appl. Mech.* **1936**, *3*, A136.
(2) Holste, J. C.; Watson, M. Q.; Bellomy, M. T.; Eubank, P. T.; Hall, K. R. *AIChE J.* **1980**, *26*, 954.
(3) Holste, J. C.; Young, J. G.; Eubank, P. T.; Hall, K. R. *AIChE J.* **1982**, *28*, 807.
(4) Ewing, M. B.; Marsh, K. N. *J. Chem. Thermodyn.* **1979**, *11*, 793.
(5) Burnett, E. S. *U.S. Bur. Mines Dept. Invest.* **1963**, 6267.
(6) Pope, G. A.; Chappelear, P.; Kobayashi, R. *Physica* **1972**, *57*, 127.
(7) Sengers, J. M. H. L.; Hastings, J. R. *Int. J. Thermophys.* **1981**, *2*, 269.
(8) Esper, G. J. Doktorarbeit, Ruhr-Universtät, Bochum, West Germany, 1987.
(9) Hall, K. R.; Eubank, P. T. *Physica* **1972**, *61*, 346.
(10) Hall, K. R.; Eubank, P. T. *AIChE J.* **1974**, *20*, 815.
(11) Hall, K. R.; Eubank, P. T. *AIChE J.* **1975**, *21*, 1111.
(12) Hall, K. R.; Eubank, P. T. *AIChE J.* **1976**, *22*, 399.
(13) Hall, K. R.; Eubank, P. T.; Holste, J. C. *Tex. Eng. Exp. Stn. Tech. Bull.* **1978**, *78–3*, 13.
(14) Bellomy, M. T. M.S. Thesis, Texas A&M University, College Station, TX, 1976.
(15) Watson, M. Q. M.S. Thesis, Texas A&M University, College Station, TX, 1978.
(16) Young, J. G. M.S. Thesis, Texas A&M University, College Station, TX, 1978.
(17) Michels, A.; Wassenaar, T.; Zwietering, J. N. *Physica* **1952**, *18*, 67.
(18) Bloomer, O. T. *Inst. Gas Tech. Res. Bull.* **1952**, *13*, 12 pages.
(19) Goodwin, R. D. *J. Res. Nat. Bur. Stand.* **1961**, *65C*, 231.
(20) Vennix, A. J.; Leland, T. W.; Kobayashi, R. *Adv. Cryogen. Eng.* **1966**, *12*, 700.
(21) Wagner, W. *Cryogenics* **1973**, *13*, 470.
(22) Thomas, W.; Zander, M. *Int. J. Thermophys.* **1980**, *1*, 383.
(23) Straty, G. C.; Palavra, A. M. F. *J. Res. Nat. Bur. Stand.* **1984**, *89*, 375.
(24) Lau, W. R. Ph.D. Dissertation, Texas A&M University, College Station, TX, 1986.
(25) Yurttaş, L. Ph.D. Dissertation, Texas A&M University, College Station, TX, 1988.
(26) Osburn, D. C., III. M.S. Thesis, Texas A&M University, College Station, TX, 1981.
(27) Childers, L. P. M.S. Thesis, Texas A&M University, College Station, TX, 1984.
(28) Holste, J. C.; Eubank, P. T.; Hall, K. R. *Ind. Eng. Chem. Fundam.* **1977**, *16*, 378.
(29) Linsky, D.; Levelt Sengers, J. M. H.; Davis, H. A. *Rev. Sci. Instrum.* **1987**, *58*, 817.
(30) Ely, J. F.; Haynes, W. M.; Bain, B. C. *J. Chem. Thermodyn.* **1989**, *21*, 879.
(31) Sengers, J. M. H. L.; Chen, W. T. *J. Chem. Phys.* **1972**, *56*, 595.

Received for review May 10, 1993. Revised March 28, 1994. Accepted April 15, 1994.* The authors appreciate financial support from the Gas Research Institute, the Gas Processors Association, and the Texas Engineering Experiment Station (TEES).

* Abstract published in *Advance ACS Abstracts*, May 15, 1994.